РАДИОФИЗИКА, ЭЛЕКТРОНИКА, АКУСТИКА

Tamm resonances control in one-dimensional microwave photonic crystal for measuring parameters of heavily doped semiconductor layers

A. V. Skripal✉ **, D. V. Ponomarev, A. A. Komarov, V. E. Sharonov**

Saratov State University, 83 Astrakhanskaya St., Saratov 410012, Russia

Alexander V. Skripal, skripala_v@info.sgu.ru, https://orcid.org/0000-0001-7448-4560
Denis V. Ponomarev, ponomarev87@mail.ru, https://orcid.org/0000-0002-7822-937X
Andrey A. Komarov, androkom86@gmail.com, https://orcid.org/0000-0002-9869-7920
Vasily E. Sharonov, 769545.1998@mail.ru, https://orcid.org/0000-0001-6035-7747

Abstract. The possibility has been explored to control the photonic Tamm resonances (TRs) in the one-dimensional microwave photonic crystal (MPC) with the dielectric filling by changing the thickness of the MPC's outer layer adjacent to the heavily doped layer of the semiconductor GaAs structure. The controlled photonic TRs have been used to measure the conductivity of the heavily doped semiconductor layer. It has been shown that depending on the conductivity of the layer the specific tuning of the TR frequency is necessary in order to achieve a high sensitivity of the TR to the change of the conductivity. The possibility of observing the plasma resonance in the infrared range has additionally allowed to determine the concentration and mobility of free charge carriers in the heavily doped layer of the GaAs structure.

Keywords: conductivity measurement, heavily doped semiconductor, microwave photonic crystals, plasma resonance, Tamm resonances, X-band

Научная статья
УДК 621.372.2

Управление таммовскими резонансами в одномерных СВЧ фотонных кристаллах для измерения параметров сильнолегированных полупроводниковых слоев

А. В. Скрипаль✉ **, Д. В. Пономарев, А. А. Комаров, В. Е. Шаронов**

Саратовский национальный исследовательский государственный университет имени Н. Г. Чернышевского, Россия, 410012, г. Саратов, ул. Астраханская, д. 83

Скрипаль Александр Владимирович, доктор физико-математических наук, профессор, заведующий кафедрой физики твердого тела, skripala_v@info.sgu.ru, https://orcid.org/0000-0001-7448-4560
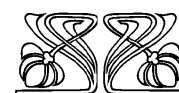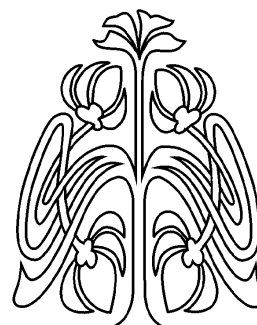
НАУЧНЫЙ ОТДЕЛ

Пономарев Денис Викторович, кандидат физико-математических наук, доцент кафедры физики твердого тела, ponomarev87@mail.ru, https://orcid.org/0000-0002-7822-937X

Комаров Андрей Александрович, аспирант кафедры физики твердого тела, androkom86@gmail.com, https://orcid.org/0000-0002-9869-7920

Шаронов Василий Евгеньевич, магистрант кафедры физики твердого тела, 769545.1998@mail.ru, https://orcid.org/0000-0001-6035-7747
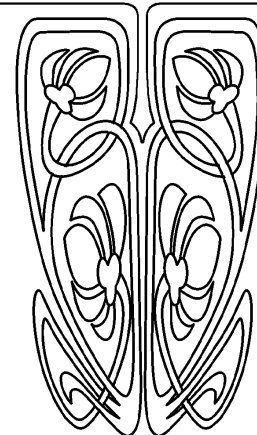
Аннотация. Исследована возможность управления фотонными таммовскими резонансами в одномерном СВЧ фотонном кристалле с диэлектрическим заполнением с помощью изменения толщины слоя фотонного кристалла, граничащего с сильнолегированным слоем полупроводниковой GaAs структуры. Управляемые фотонные таммовские резонансы в микроволновом диапазоне частот использованы для измерения удельной электропроводности сильнолегированных полупроводниковых слоёв. Показано, что для достижения высокой чувствительности таммовского резонанса к изменению удельной электропроводности сильнолегированного слоя, необходима определенная перестройка частоты таммовского резонанса, величина которой определяется величиной удельной электропроводности сильнолегированного слоя. Возможность наблюдения плазменного резонанса в инфракрасном диапазоне позволило определить концентрацию и подвижность свободных носителей заряда в сильнолегированном слое полупроводниковой GaAs структуры.

Ключевые слова: измерение проводимости, сильно легированный полупроводник, СВЧ фотонные кристаллы, плазменный резонанс, таммовские резонансы, X-диапазон

Introduction

One of the directions in the development of microwave technology is the creation of microwave components based on periodic structures called Bragg microwave structures or microwave photonic crystals (MPC) [1–5]. The appearance of resonances (defect modes) in MPC due to the introduction of elements that disturb the periodicity of the MPC makes it possible to create measurement techniques of the material parameters and structures in the microwave range.

The materials and samples under test, such as dielectrics, polar liquids, composites, and structures with semiconductor layers, are generally inserted inside the MPC, most commonly in its central layer [1, 6–9].

However, this method has a number of limitations associated with the almost complete disappearance of the defect mode in the MPC's band gap when the samples characterized by high losses are introduced into the MPC. The disappearance of the defect mode is observed, for example, at the measurement of the samples containing thin highly conducting nanolayers.

Thin highly conducting layers are used in a wide range of microwave technology applications. Microwave matched loads, bolometric power meters of the millimeter and sub-terahertz ranges, electromagnetic shields, and elements of integrated microwave circuits are created on their basis [10–16]. Highly conducting films, created using various conducting ink printing technologies, are essential elements of flexible electronics and photonics with large areas [17–26].

The studies of thin conducting layers using transmission line methods [27–30], as a rule, are based on the transmission/reflection coefficient measurement. The range of measured thicknesses and conductivities is determined by the dynamical range of the measured transmission/reflection coefficients of the used measuring system. For implementing resonator measurement methods [27, 31, 32], which provide a wider range of measured thicknesses and conductivities, it becomes necessary to create a precision high-Q resonator and carry out its preliminary calibration without a sample.

One of the approaches providing measurements of highly conducting layers in the microwave range is the use of surface states in MPCs. The approach was successfully applied to measure the conductivity of metal nanolayers [33]. However, the measurement ranges of the thickness and conductivity are limited due to the fact that the pronounced Tamm resonance (TR) is observed only at specific values of the thickness and conductivity of the metal nanolayer.

In this work, we have developed an approach aimed at solving the problem of diagnostics of conducting layers with high and extremely high conductivity, which are used in various fields of microwave technology. This is especially important for diagnostics of conducting graphene structures with thicknesses of several nanometers as well as heavily doped semiconductor layers with thicknesses from tens of nanometers to several micrometers.

To achieve this goal, it is proposed to tune the Tamm resonance's frequency in the MPC depending on the thickness and conductivity of the conducting layers under test.

The possibility to tune the frequency and amplitude of the TR in the optical range was demonstrated in a number of works [34–39].

Note, that in contrast to the optical range, in which the tuning of the TR can be carried out both by a change of the conductivity and thickness of the conducting layer, and by a change of the parameters of the photonic crystal, in the MPC, a change of the conductivity and thickness of the conducting layer does not change the frequency of the TR, but only its amplitude.

In this regard, in order to observe a pronounced TR at different values of the conductivity and thickness of the conducting layer, we have implemented a frequency control procedure of the TR in the MPC by changing the thickness of the outer layer of the MPC adjacent to the conducting layer.

1. Computer simulation of controlling the TR characteristics

The MPC assembled from Al_2O_3 ceramic (the odd positions, $\varepsilon = 9.6$, the thickness – 0.5 mm) and teflon (the even positions, $\varepsilon = 2.0$, the thickness – 18 mm) layers has been tested in the range 7–13 GHz. The MPC consisted of 11 layers; the thickness of the one of the outer layers is varied.

The semiconductor structure under test consisted of three gallium arsenide GaAs layers. The semiconductor structure was placed behind the MPC in such a way that the highly doped epitaxial n^+-layer was directly adjacent to its outer dielectric layer. In this case, two configurations were considered: the thickness of the MPC's outer layer adjacent to the n^+-layer of the GaAs structure d_L was 0.5 mm (configuration *1* in Fig. 1), the thickness of the MPC's outer layer adjacent to the n^+-layer of the GaAs structure d_L was 1.0 mm (configuration *2* in Fig. 1).

To find out the possibility to solve the problem of measuring thin conducting layers with high and extremely high conductivity using frequency-controlled TRs, the transmission (S_{21}) and reflection (S_{11}) coefficients of the MPC containing a semiconductor structure with a conductivity of the n^+-layer $0.8 \cdot 10^5$ $\Omega^{-1}m^{-1}$ and $1.6 \cdot 10^5$ $\Omega^{-1}m^{-1}$ were calculated (Fig.2).
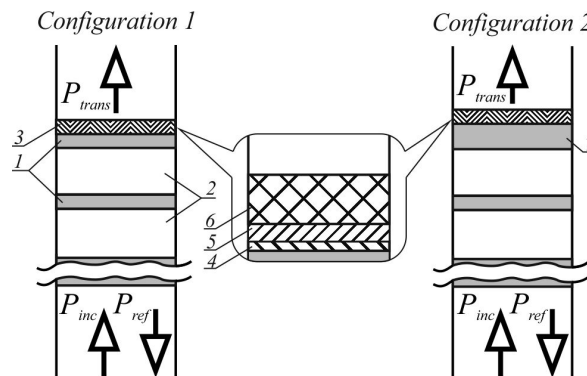
Fig. 1. Design of the one-dimensional waveguide MPC with the semiconductor n^+-n-i-structure: *1* – ceramic layer, *2* – teflon layer, *3* – n^+-n-i-structure, *4, 5, 6* – n^+, n and *i*-layers, *7* – outer layer (ceramic) of the photonic crystal with the changed thickness, adjacent to the n^+-layer
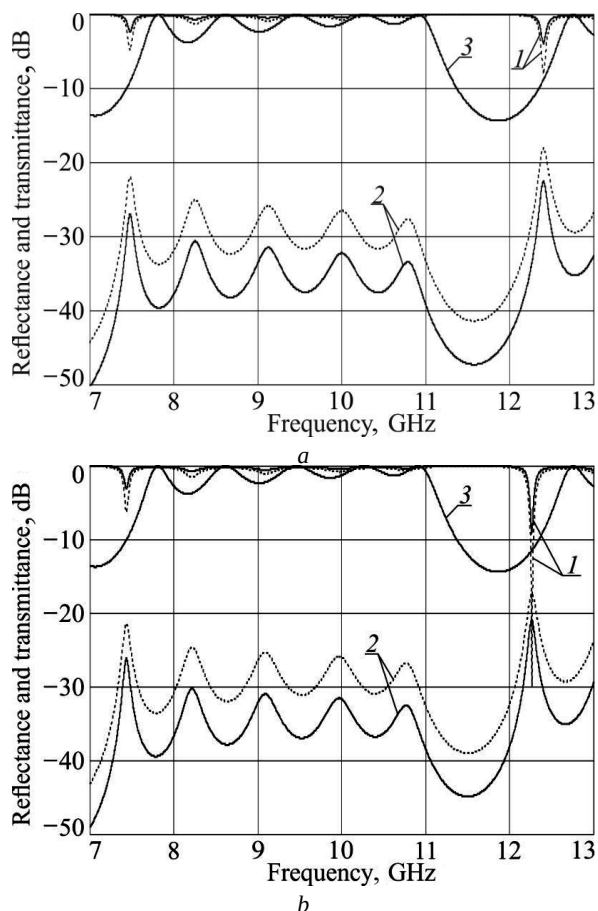
Fig. 2. Calculated S_{11} (curves *1*), S_{21} (curves *2*) of the MPC adjacent to the n^+-layer of the semiconductor structure with the conductivity equal to $0.8 \cdot 10^5$ $\Omega^{-1}m^{-1}$ (solid curves) and $1.6 \cdot 10^5$ $\Omega^{-1}m^{-1}$ (dashed curves) for two thicknesses d_L of the MPC's outer layer: *a* – 0.5 mm, *b* – 1 mm. S_{21} of the MPC without the semiconductor structure is curve *3*

The coefficients S_{11} and S_{21} were calculated by the transfer matrix method with allowance for only the fundamental H_{10} wave type propagation in the waveguide [33, 40, 41].

The frequency of the TR was controlled by varying the thickness of the MPC's outer Al_2O_3 ceramic layer adjacent to the n^+-layer.

As follows from the calculation results, for the thickness d_L of the MPC's outer layer adjacent to the n^+-layer of the GaAs structure equal to 0.5 mm (this is the thickness of all odd layers of the MPC), two resonances appear at frequencies $f_{\text{Tamm1}} = 7.476$ GHz and $f_{\text{Tamm2}} = 12.4$ GHz. When the conductivity of the n^+-layer changes in the range from 0.8×10^5 $\Omega^{-1}\text{m}^{-1}$ to $1.6 \cdot 10^5$ $\Omega^{-1}\text{m}^{-1}$, the change of S_{11} and S_{21} at the TR frequency f_{Tamm1} is 2.4 dB and 5.0 dB, and at f_{Tamm2} it is 4.1 dB and 4.5 dB, respectively. It should be noted that for the chosen parameters of the GaAs structure's layers, S_{21} and S_{11} are mainly determined by the parameters of the n^+-layer.

With a thickness $d_L = 1.0$ mm, the frequencies are $f_{\text{Tamm1}} = 7.432$ GHz and $f_{\text{Tamm2}} = 12.262$ GHz. At the frequency $f_{\text{Tamm2}} = 12.262$ GHz with an increase in the conductivity of the n^+-layer in the range from $0.8 \cdot 10^5$ $\Omega^{-1}\text{m}^{-1}$ to $1.6 \cdot 10^5$ $\Omega^{-1}\text{m}^{-1}$, the change of S_{11} exceeds 20.0 dB, while the change of S_{21} remains at the level of 3.5 dB.

Thus, the results of computer simulation demonstrate that the frequency tuning of the TR in the MPC can be implemented by choosing the thickness of the outer Al_2O_3 ceramics layer of the MPC adjacent to the n^+-layer. In this case, the tuning of the TR frequency, which provides a high sensitivity of the TR to the change of the conductivity of the heavily doped layer, is determined by the conductivity value of this layer.

2. Use of controlled TRs in the 1D MPC for measuring the parameters of the heavily doped semiconductor layer

The experimental MPC created according to the described above model was tested for the frequency range 7–13 GHz.

For the experimental observation of the TRs, the epitaxial semiconductor structure made of gallium arsenide (GaAs) was used. It consisted of three layers: n^+, n and i-layers with the thicknesses of 1.8 μm, 11.4 μm, and 473.8 μm. The tested semiconductor structure was placed behind the MPC. The highly doped epitaxial layer was directly adjacent to its outer dielectric layer (Fig. 3).

To experimentally confirm the possibility of tuning the TR frequency, which provides a high sensitivity of the TR to the change of the conductivity of the heavily doped layer, two configurations were considered: $d_L = 0.494$ mm (configuration *1* in Fig. 1), $d_L = 0.973$ mm (configuration *2* in Fig. 1).
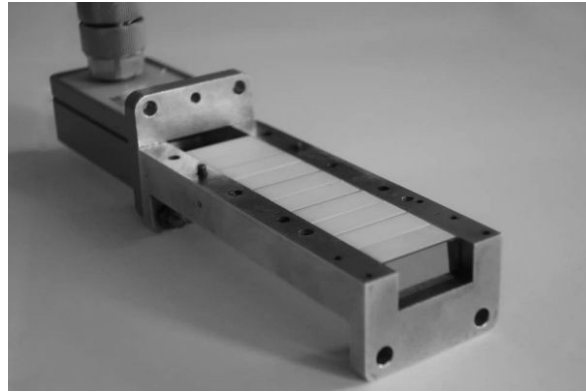

Fig. 3. The experimental waveguide section with the MPC and the tested layered GaAs sample

The experimentally obtained coefficients S_{11} and S_{21} of the MPC with the epitaxial semiconductor structure for two configurations, performed by the network analyzer Agilent PNA-X N5242A, are presented in Fig. 4.
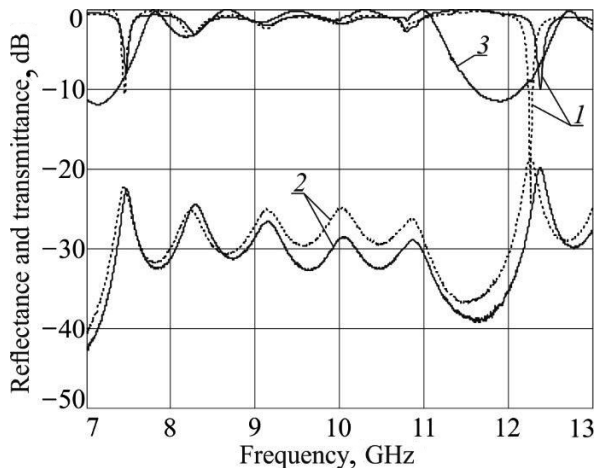
Fig. 4. Experimental S_{11} (curves *1*) and S_{12} (curves *2*) of MPCs with the three-layer GaAs structure for two different configurations: solid curves – $d_L = 0.494$ mm; dotted curves – $d_L = 0.973$ mm. S_{21} of the MPC without the semiconductor structure is curve *3*

As follows from the experiment at the thickness $d_L = 0.973$ mm of the MPC's outer layer, the resonances are characterized by a low value of the S_{11} at frequencies $f_{\text{Tamm1}} = 7.472$ GHz and $f_{\text{Tamm2}} = 12.396$ GHz. In this case, the depth and frequency of TRs are controlled by the thickness of the MPC's outer layer adjacent to the n^+-layer of the GaAs structure. This is in good agreement with the presented above calculation results and demonstrates the possibility to tune the frequency of the photonic TR to achieve a high sensitivity of the TR to changes of the conductivity of the heavily doped layer. In this case, the required value of the frequency tuning is determined by the conductivity value of this heavily doped layer.

The implementation of the highly sensitive TR makes it possible to use the method based on the measurement of S_{21} and S_{11} of the MPC containing the structure under test to determine the conductivity of the highly doped epitaxial semiconductor n^+-layer [33].

The sought value of the conductivity σ_{n+} of the n^+-layer is defined numerically by the least squares method from solving the equation:

$$\frac{\partial \delta(\sigma_+)}{\partial \sigma_{n^+}} = 0. \tag{1}$$

Here

$$\delta(\sigma_{n^+}) = \sum_{i=1}^{K} \left[\begin{array}{c} \left(\left| S_{21}\left(\sigma_{n^+}, f_{\exp_i}\right) \right|^2 - \left| S_{21\exp_i} \right|^2 \right)^2 + \\ + \left(\left| S_{11}\left(\sigma_{n^+}, f_{\exp_i}\right) \right|^2 - \left| S_{11\exp_i} \right|^2 \right)^2 \end{array} \right], \tag{2}$$

where $S_{21\exp}$, $S_{11\exp}$ are the experimental and $S_{21}(\sigma_{n+}, f)$, $S_{11}(\sigma_{n+}, f)$ calculated transmission and reflection coefficients.

Using the results of measuring S_{21} and S_{11} in the vicinity of the TR frequency $f_{\text{Tamm2}} = 12.396$ GHz at the thickness $d_L = 0.973$ mm of the MPC' outer layer, the value of the conductivity σ_{n+} of the highly doped epitaxial GaAs layer with the thickness 1.8 μm has been determined as $0.843 \cdot 10^5$ $\Omega^{-1}\text{m}^{-1}$ by solving the inverse problem.

The measured S_{21}, S_{11} and calculated ones by using the obtained value $\sigma_{n+} = 0.843 \cdot 10^5$ $\Omega^{-1}\text{m}^{-1}$ of the highly doped epitaxial GaAs layer agree well as shown in Fig. 5.
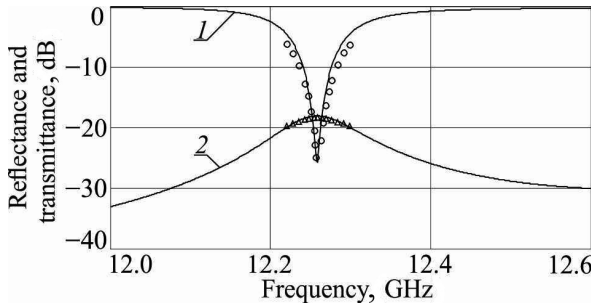
Fig. 5. Measured (points) and calculated (curves) S_{11} (curve *1*) and S_{21} (curve *2*) by using the obtained value of the conductivity $0.843 \cdot 10^5$ $\Omega^{-1}\text{m}^{-1}$ of the MPC with the tested GaAs structure

To evaluate the correctness of the results, obtained by the method using the photonic TRs, the conductivity measurements were carried out by an independent method. A four-probe method based on the measurement of the surface resistance ρ was used as an alternative independent method for measuring the conductivity σ_{n+} of the GaAs n^+-layer. The conductivity, at known thickness d of the GaAs n^+-layer,

is obtained from the well-known relation:

$$\sigma_{n^+} = \frac{1}{\rho \cdot d}. \tag{3}$$

The measured by the Jandel RMS-EL-Z probe station value of the surface resistance ρ was 7Ω per square, which corresponds to the value of the conductivity equal to $0.794 \cdot 10^5$ $\Omega^{-1}\text{m}^{-1}$ with the n^+-layer thickness $d = 1.8$ μm.

Thus, the difference between the results of measuring the conductivity of the highly doped GaAs n^+-layer using the microwave TRs and the surface resistance is no more than 6.2%. It should be noted that the relative error in measuring the surface resistance of highly conducting layers in the selected range of resistance values by the four-probe method can reach 14%.

For the heavily doped semiconductor structures with high electron mobility it is possible to observe a pronounced plasma resonance in the infrared range. This provides the possibility of obtaining the concentration n^+ of free charge carriers from measurements of the plasma resonance frequency ω_p using the relation [42]:

$$n^+ = \frac{m^* \varepsilon_0 \varepsilon_L (\omega_p)^2}{e^2}, \tag{4}$$

where m^* is the effective mass of free charge carriers, depending on their concentration at a high doping level [43], ε_L is the permittivity of the crystal lattice in the infrared range [43].

In the infrared range from 350 to 7800 cm^{-1}, the reflection coefficient of the tested GaAs structure was measured using the Shimadzu IRAffinity-1S spectrophotometer (Fig. 6).
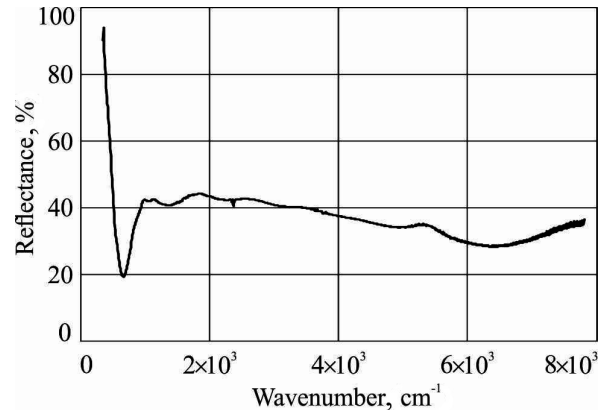
Fig. 6. Reflection coefficient of the tested layered GaAs sample in the infrared range

As follows from the measurement results, the plasma frequency, defined as $\omega_p = 2\pi c/\lambda_p$ is equal to $1.192 \cdot 10^{14}$ rad/s. Here $\lambda = \lambda_{\min}\left[(\varepsilon_L - 1)/\varepsilon_L\right]^{1/2}$,

where $\lambda_{\min}$ is the wavelength in the minimum of the reflection coefficient in the infrared range.

Using the obtained value of the plasma frequency $\omega_p = 1.192 \cdot 10^{14}$ rad/s and the expression (4), the concentration has been determined as $n^+ = 3.9 \cdot 10^{24}$ m^{-3}. The permittivity of the GaAs crystal lattice in the infrared range was chosen equal to 10.89, the effective mass of charge carriers in GaAs at this doping level was $0.078 \cdot m_e$, where m_e is the mass of a free electron.

To determine the free charge carriers mobility μ in the tested GaAs n^+-layer the well-known relation $\mu = \sigma_{n+}/(en^+)$, where n^+ is the concentration of free charge carriers, was used. The calculated value of the mobility 0.134 m^2/(V·s) correlates well with the values known from the literature for heavily doped GaAs layers [43, 44].

To evaluate the correctness of the results of the mobility measurement using the photonic TRs and plasma resonance, the mobility was measured independently by the well-known method of microwave magnetoresistance [45, 46].

In this method, the mobility is obtained from the measured attenuation α_m and α of the microwave signal in the waveguide section containing the GaAs structure with and without external magnetic field B, respectively:

$$\mu = \frac{1}{B}\sqrt{\frac{\alpha - \alpha_m}{\alpha_m}}. \qquad (5)$$

The value of the mobility of charge carriers measured using this method was 0.129 m^2/(V·s).

The difference between the results of measuring μ using the conductivity obtained by the method of microwave TRs and by the methods of plasma resonance and magnetoresistance is no more than 4.0%.

Thus, the use of controlled TRs in the one-dimensional MPCs and the additional observation of the plasma resonance in the infrared range in the tested semiconductor structure makes it possible to implement along with the conductivity measurement technique the method for determining the concentration of charge carriers and their mobility.

Conclusion

Thus, the approach aimed at solving the problem of measuring thin highly conducting layers with high and extremely high conductivity, which are used in various fields of microwave technology as absorbers of electromagnetic radiation, bolometric power meters in the millimeter and subterahertz ranges, electromagnetic shields, elements of electronics and photonics with large areas, has been developed in this work.

To achieve this goal, it is proposed to tune the TR's frequency in the MPC depending on the thickness and conductivity of the conducting layers under test. The control of the TR in the MPC is provided by the change of the thickness of the outer layer of the MPC adjacent to the conducting layer. In this case, the required frequency tuning value is determined by the value of the conductivity of the conducting layer. The applicability of the developed approach has been confirmed by the example of measuring heavily doped semiconductor layers.

The developed method can also find application for diagnostics of microwave microfluidic circuits, flexible and stretchable antennas for biointegrated electronics [47–49].

References

1. Usanov D. A., Nikitov S. A., Skripal A. V., Ponomarev D. V. *One-dimensional Microwave Photonic Crystals : New Applications.* CRC Press, Taylor Francis Group, 2019. 154 p. https://doi.org/10.1201/9780429276231

2. Belyaev B. A., Khodenkov S. A., Shabanov V. F. Investigation of frequency-selective devices based on a microstrip 2D photonic crystal. *Doklady Physics* [Physics Reports], 2016, vol. 61, no. 4, pp. 155–159. https://doi.org/10.1134/S1028335816040017

3. Fernandes H. C. C., Medeiros J. L. G., Junior I. M. A., Brito D. B. Photonic crystal at millimeter waves applications. *PIERS Online*, 2007, vol. 3, no. 5, pp. 689–694. https://doi.org/10.2529/PIERS060901105337

4. El-Shaarawy H. B., Coccetti F., Plana R., El-Said M., Hashish E. A. Defected ground structures (DGS) and uniplanar compact-photonic band gap (UC-PBG) structures for reducing the size and enhancing the out-of-band rejection of microstrip bandpass ring resonator filters. *WSEAS Trans. on Comm.*, 2008, vol. 7, no. 11, pp. 1112–1121.

5. Yao J., Yuan C., Li H., Wu J., Wang Y., Kudryavtsev A. A., Demidov V. I., Zhou Z. 1D photonic crystal filled with low-temperature plasma for controlling broadband microwave transmission. *AIP Advances*, 2019, vol. 9, no. 6, article no. 065302. https://doi.org/10.1063/1.5097194

6. Usanov D. A., Skripal A. V., Abramov A. V., Bogolyubov A. S., Kulikov M. Yu., Ponomarev D. V. Microstrip photonic crystals used for measuring parameters of liquids. *Tech. Phys.*, 2010, vol. 55, no. 8, pp. 1216–1221. https://doi.org/10.1134/S1063784210080220

7. Usanov D. A., Skripal A. V., Romanov A. V. Complex permittivity of composites based on dielectric matrices with carbon nanotubes. *Tech. Phys.*, 2011, vol. 56, no. 1, pp. 102–106. https://doi.org/doi.org/10.1134/S1063784211010257

8. Usanov D. A., Nikitov S. A., Skripal A. V., Ponomarev D. V., Latysheva E. V. Photonic band gap structures and their application for measuring parameters of semiconductor layers. *Proc. of the IEEE MTT-S Int. Microw. Symp. (IMS)*, 2015, pp. 1–4. https://doi.org/10.1109/MWSYM.2015.7166794

9. Usanov D. A., Skripal A. V., Ponomarev D. V., Ruzanov O. M., Timofeev I. O., Nikitov S. A. Application of a microwave coaxial Bragg structures for the measurement of parameters of insulators. *J. Commun. Technol.*, 2020, vol. 65, no. 5, pp. 541–548. https://doi.org/10.1134/S1064226920040087

10. Usanov D. A., Skripal A. V., Abramov A. V., Bogolubov A. S., Skvortsov V. S., Merdanov M. K. Wideband waveguide matched loads based on photonic crystals with nanometer metal layers. *Proc. of 38th Eur. Microw. Conf. (EuMC)*, 2008, pp. 484–487. https://doi.org/10.1109/EUMC.2008.4751494

11. Usanov D. A., Meshchanov V. P., Skripal A. V., Popova N. F., Ponomarev D. V., Merdanov M. K. Centimeter- and millimeter-wavelength matched loads based on microwave photonic crystals. *Tech. Phys.*, 2017, vol. 62, no. 2, pp. 243–247. https://doi.org/10.1134/S106378421702027X

12. Li S., Luo J., Anwar S., Li S., Lu W. Hong Hang Z., Lai Y., Hou B., Shen M., Wang C. Broadband perfect absorption of ultrathin conductive films with coherent illumination : Superabsorption of microwave radiation. *Phys. Rev. B*, 2015, vol. 91, no. 22, article no. 220301(R). https://doi.org/10.1103/PhysRevB.91.220301

13. Costa D. S., Nohara E. L., Rezende M. C. Comparative study of experimental and numerical behaviors of microwave absorbers based on ultrathin Al and Cu films. *Mater. Chem. Phys.*, 2017, vol. 194, pp. 322–326. https://doi.org/10.1016/j.matchemphys.2017.03.056

14. Ou M., Qiu W., Huang K., Chu S. Ultra-flexible and high-performance electromagnetic wave shielding film based on CNTF/liquid metal composite films. *J. Appl. Phys.*, 2019, vol. 125, no. 13, article no. 134906. https://doi.org/10.1063/1.5089579

15. Asmatulu R., Bollavaram P. K., Patlolla V. R., Alarifi I. M., Khan W. S. Investigating the effects of metallic submicron and nanofilms on fiber-reinforced composites for lightning strike protection and EMI shielding. *Adv. Compos. Hyb. Mater.*, 2020, vol. 3, no. 1, pp. 66–83. https://doi.org/10.1007/s42114-020-00135-7

16. Bengio E. A., Senic D., Taylor L. W., Headrick R. J., King M., Chen P., Little C. A., Ladbury J., Long C. J., Holloway C. L., Babakhani A., Booth J. C., Orloff N. D., Pasquali M. Carbon nanotube thin film patch antennas for wireless communications. *Appl. Phys. Lett.*, 2019, vol. 114, no. 20, article no. 203102. https://doi.org/10.1063/1.5093327

17. Parashkov R., Becker E., Riedl T., Johannes H. H., Kowalsky W. Large area electronics using printing methods. *Proc. IEEE*, 2005, vol. 93, no. 7, pp. 1321–1329. https://doi.org/10.1109/JPROC.2005.850304

18. Perelaer J., Smith P., Mager D., Soltman D., Volkman S. K., Subramanian V., Korvink J. G., Schubert U. S. Printed electronics : The challenges involved in printing devices, interconnects, and contacts based on inorganic materials. *J. Mater. Chem.*, 2010, vol. 20, no. 39, pp. 8446–8453. https://doi.org/10.1039/C0JM00264J

19. Räisänen A., Ala-Laurinaho J., Asadchy V., Diaz-Rubio A., Khanal S., Semkin V., Tretyakov S., Wang X., Zheng J., Alastalo A., Mäkelä T., Sneck A. Suitability of roll-to-roll reverse offset printing for mass production of millimeter-wave antennas : Progress report. *Proc. Antennas Propag. Conf. (LAPC)*, 2016, pp. 300–304. https://doi.org/10.1109/LAPC.2016.7807528

20. Moonen P. F., Yakimets I., Huskens J. Fabrication of transistors on flexible substrates : From mass-printing to high-resolution alternative lithography strategies. *Adv. Mater.*, 2012, vol. 24, no. 41, pp. 5526–5541. https://doi.org/10.1002/adma.201202949

21. Khan S., Lorenzelli L., Dahiya R. S. Technologies for printing sensors and electronics over large flexible substrates : A review. *IEEE Sens. J.*, 2015, vol. 15, no. 6, pp. 3164–3185. https://doi.org/10.1109/JSEN.2014.2375203

22. Krebs F. C. Fabrication and processing of polymer solar cells : A review of printing and coating techniques. *Sol. Energy Mater. Sol. Cells*, 2009, vol. 93, no. 4, pp. 394–412. https://doi.org/10.1016/j.solmat.2008.10.004

23. Clemens W., Fix W., Ficker J., Knobloch A., Ullmann A. From polymer transistors toward printed electronics. *J. Mater. Res.*, 2004, vol. 19, no. 7, pp. 1963–1973. https://doi.org/10.1557/JMR.2004.0263

24. Khan Y., Thielens A., Muin S., Ting J., Baumbauer C., Arias A. C. A New Frontier of Printed Electronics : Flexible Hybrid Electronics. *Adv. Mater.*, 2019, vol. 32, no. 15, article no. 1905279. https://doi.org/10.1002/adma.201905279

25. Li D., Lai W.-Y., Zhang Y.-Z., Huang W. Printable Transparent Conductive Films for Flexible Electronics. *Adv. Mater.*, 2018, vol. 30, no. 10, article no. 1704738. https://doi.org/10.1002/adma.201704738

26. Kim D., Moon J. Highly conductive ink jet printed films of nanosilver particles for printable electronics. *Electrochem. Solid-State Lett.*, 2005, vol. 8, no. 11, pp. J30–J33. https://doi.org/10.1149/1.2073670

27. Chen L. F., Ong C. K., Neo C. P., Varadan V. V., Varadan V. K. *Microwave Electronics : Measurement and Materials Characterization.* Chichester, West Sussex, England, John Wiley & Sons Ltd, 2004. 537 p. https://doi.org/10.1002/0470020466

28. Lee M.-H. J., Collier R. J. Sheet resistance measurement of thin metallic films and stripes at both 130 GHz and DC. *IEEE Trans. Instrum. Meas.*, 2005, vol. 54, no. 6, pp. 2412–2415. https://doi.org/10.1109/TIM.2005.858536

29. Poo Y., Wu R.-X., Fan X., Xiao J. Q. Measurement of ac conductivity of gold nanofilms at microwave frequencies. *Rev. Sci. Instrum.*, 2010, vol. 81, no. 6, article no. 064701. https://doi.org/10.1063/1.3436450

30. Wang X.-C., Díaz-Rubio A., Tretyakov S. A. An accurate method for measuring the sheet impedance of thin conductive films at microwave and millimeter-wave frequencies. *IEEE Trans. Microw. Theory Techn.*, 2017, vol. 65, no. 12, pp. 5009–5018. https://doi.org/10.1109/TMTT.2017.2714662

31. Krupka J., Strupinski W., Kwietniewski N. Microwave conductivity of very thin graphene and metal films. *J. Nanosci. Nanotechnol.*, 2011, vol. 11, no. 4, pp. 3358–3362. https://doi.org/10.1166/jnn.2011.3728

32. Krupka J., Mazierska J. Contactless measurements of resistivity of semiconductor wafers employing single-post and split-post dielectric-resonator techniques. *IEEE Trans. Instrum. Meas.*, 2007, vol. 56, no. 5, pp. 1839–1844. https://doi.org/10.1109/TIM.2007.903647

33. Skripal A. V., Ponomarev D. V., Komarov A. A. Tamm resonances in the structure 1-D microwave photonic crystal / conducting nanometer layer. *IEEE Trans. Microw. Theory Techn.*, 2020, Dec., vol. 68. no. 12, pp. 5115–5122. https://doi.org/10.1109/TMTT.2020.3021412

34. Gazzano O., Vasconcellos S. M. de, Gauthron K., Symonds C., Bloch J., Voisin P., Bellessa J., Lemaître A., Senellart P. Evidence for confined Tamm plasmon modes under metallic microdisks and application to the control of spontaneous optical emission. *Phys. Rev. Lett.*, 2011, vol. 107, no. 24, article no. 247402. https://doi.org/10.1103/PhysRevLett.107.247402

35. Zhou H., Yang G., Wang K., Long H., Lu P. Multiple optical Tamm states at a metal-dielectric mirror interface. *Opt. Lett.*, 2010, vol. 35, no. 24, pp. 4112–4114. https://doi.org/10.1364/OL.35.004112

36. Chang C. Y., Chen Y. H., Tsai Y. L., Kuo H. C., Chen K. P. Tunability and optimization of coupling efficiency in Tamm plasmon modes. *IEEE Journal of Selected Topics in Quantum Electronics*, 2015, July–Aug., vol. 21, no. 4, pp. 262–267, article no. 4600206. https://doi.org/10.1109/JSTQE.2014.2375151

37. Isić G., Vuković S. Jakšić Z., Belić M. Tamm plasmon modes on semi-infinite metallodielectric superlattices. *Sci. Rep.*, 2017, vol. 7, no. 1, article no. 3746. https://doi.org/10.1038/s41598-017-03497-z

38. Cheng H.-C., Kuo C.-Y., Hung Y.-J., Chen K.-P., Jeng S.-C. Liquid-crystal active Tamm-plasmon devices. *Phys. Rev. Appl.*, 2018, vol. 9, no. 6, article no. 064034. https://doi.org/10.1103/PhysRevApplied.9.064034

39. Jeng S.-C. Applications of Tamm plasmon-liquid crystal devices. *Liquid Crystals*, 2020, vol. 47, no. 8, pp. 1–9. https://doi.org/10.1080/02678292.2020.1733114

40. Usanov D. A., Skripal A. V., Abramov A. V., Bogolyubov A. S. Microwave measurements of thickness of nanometer metal layers and conductivity of semiconductor in structures 'metal-semiconductor. *Proceedings of the XVI International Conference on Microwaves, Radar and Wireless Communications MIKON-2006.* 2006, vol. 3, pp. 874–877. https://doi.org/10.1109/MIKON.2006.4345379

41. Usanov D. A., Skripal A. V., Abramov A. V., Bogolyubov A. S., Kalinina N. V. Measurements of thickness of metal films in sandwich structures by the microwave reflection spectrum. *Proc. of 36th Eur. Microw. Conf. (EuMC)*, 2006, pp. 921–924. https://doi.org/10.1109/EUMC.2006.281071

42. Seeger K. *Semiconductor Physics : An Introduction.* Springer-Verlag, 2004. 538 p. https://doi.org/10.1007/978-3-662-09855-4

43. Blakemore J. S. Semiconducting and other major properties of gallium arsenide. *J. Appl. Phys.*, 1982, vol. 53, no. 10, pp. R123–R181. https://doi.org/10.1063/1.331665

44. Sotoodeh M., Khalid A. H., Rezazadeh A. A. Empirical low-field mobility model for III–V compounds applicable in device simulation codes. *J. Appl. Phys.*, 2000, vol. 87, no. 6, pp. 2890–2900. https://doi.org/10.1063/1.372274

45. Molnar B., Kenedy T. A. Evaluation of S- and Se-implanted GaAs by contactless mobility measurement. *Journal of Electrochemical Society : Solid-state Science and Technology*, 1978, vol. 125, no. 8, pp. 1318–1320. https://doi.org/10.1149/1.2131670

46. Usanov D. A., Nikitov S. A., Skripal A. V., Ponomarev D. V., Latysheva E. V. Multiparametric measurements of epitaxial semiconductor structures with the use of one-dimensional microwave photonic crystals. *J. Commun. Technol.*, 2016, vol. 61, no. 1, pp. 42–49. https://doi.org/10.1134/S1064226916010125

47. Bo G., Ren L., Xu X., Du Y., Dou S. Recent progress on liquid metals and their applications. *Adv. Phys. : X*, 2018, vol. 3, no. 1, pp. 411–442. https://doi.org/10.1080/23746149.2018.1446359

48. Xie Z., Avila R., Huang Y., Rogers J. A. Flexible and Stretchable Antennas for Biointegrated Electronics. *Adv. Mater.*, 2019, vol. 32, no. 15, article no. 1902767. https://doi.org/10.1002/adma.201902767

49. Bakar H. A., Rahim R. A., Soh P. J., Akkaraekthalin P. Liquid-Based Reconfigurable Antenna Technology : Recent Developments, Challenges and Future. *Sensors*, 2021, vol. 21, no. 3, article no. 827. https://doi.org/10.3390/s21030827